

## Effects of upstream two-dimensional hills on design wind loads: A computational approach

G. Bitsuamlak

*RWDI Inc., Guelph, Ontario, Canada*

T. Stathopoulos<sup>†</sup>

*Centre for Building Studies, Concordia University, Montreal, Quebec, Canada*

C. Bédard

*ETS-Ecole de Technologie Supérieure, Montreal, Quebec, Canada*

*(Received June 7 2004, Accepted December 22, 2005)*

**Abstract.** The paper describes a study about effects of upstream hills on design wind loads using two mathematical approaches: Computational Fluid Dynamics (CFD) and Artificial Neural Network (NN for short). For this purpose CFD and NN tools have been developed using an object-oriented approach and C++ programming language. The CFD tool consists of solving the Reynolds time-averaged Navier-Stokes equations and  $k-\varepsilon$  turbulence model using body-fitted nearly-orthogonal coordinate system. Subsequently, design wind load parameters such as speed-up ratio values have been generated for a wide spectrum of two-dimensional hill geometries that includes isolated and multiple steep and shallow hills. Ground roughness effect has also been considered. Such CFD solutions, however, normally require among other things ample computational time, background knowledge and high-capacity hardware. To assist the end-user, an easier, faster and more inexpensive NN model trained with the CFD-generated data is proposed in this paper. Prior to using the CFD data for training purposes, extensive validation work has been carried out by comparing with boundary layer wind tunnel (BLWT) data. The CFD trained NN (CFD-NN) has produced speed-up ratio values for cases such as multiple hills that are not covered by wind design standards such as the Commentaries of the National Building Code of Canada (1995). The CFD-NN results compare well with BLWT data available in literature and the proposed approach requires fewer resources compared to running BLWT experiments.

**Keywords:** computational fluid dynamics; hills; neural network; speed-up ratio; turbulence; wind load; wind velocity.

---

### 1. Introduction

Wind pressures on buildings and other structures, pedestrian level winds, and wind-induced dispersion of pollutants in urban locations depend, among other factors, on the velocity profile and

---

<sup>†</sup> Professor, Corresponding Author, E-mail: [statho@cbs-engr.concordia.ca](mailto:statho@cbs-engr.concordia.ca)

turbulence characteristics of the upcoming wind. These, in turn, depend on the roughness and general configuration of the upstream terrain. Consequently, wind standards and codes of practice typically assume upstream terrain of homogeneous roughness or provide explicit corrections for specific topographies such as a single hill or escarpment; for more complex situations they refer the practitioner to physical simulation in a boundary layer wind tunnel. The evolution of computational wind engineering makes numerical evaluation of wind velocities over complex terrain an attractive proposition. In fact, significant progress has been made in the application of Computational Fluid Dynamics (CFD) for specific cases of evaluation of wind flow over escarpments, hills as well as valleys (for representative references see, Bergeles 1985, Paterson and Holmes 1993, Maurizi 2000, Bitsuamlak, *et al.* 2003, Lun, *et al.* 2003, and Chung and Bienkiewicz 2004). Bitsuamlak, *et al.* (2004) have also reviewed the state-of-the-art on numerical wind flow simulation over complex terrain. At present, utilization of numerical simulations to predict wind speed-up in practical applications is rather limited and designers still have to rely on physical simulations for complex terrain situations. This is mainly due to the unavailability of specialized and cost-effective numerical tools targeted to give solutions for wind flow over different topographies. Hence the present objective is to develop a specialized numerical tool fine-tuned for the application of wind flow simulation over different types of terrain. To this end special emphasis is given to incorporate influential parameters such as the ground roughness. Body-fitted coordinates are used to represent the terrain accurately. An orthogonal grid generator suitable for the present type of study, which is characterized by curved and slopping surfaces, has also been developed.

The complexity generally associated with CFD-based numerical tools requires background knowledge and experience, fast hardware with large memory, and availability of ample computational time. Thus in parallel to developing such numerical tools, simple ways must be devised to convey the results produced by the complex CFD simulations to the engineering profession (end-user). To this effect, the authors have proposed and developed a NN model trained with CFD-generated data. The proposed NN model is capable of producing speed-up ratio values following input of simple geometrical parameters describing the topography and roughness of the ground. Many applications of NN in engineering have been reported in the literature, although only few have been reported in Wind Engineering. Sandri and Mehta (1995) first demonstrated the use and adaptability of NN to wind-induced damage predictions. Khanduri, *et al.* (1995, 1997) suggested a NN approach for the assessment of wind-induced interference effects on design loads for buildings. English and Fricke (1999) described a NN application for analysis of interference index. Bitsuamlak, *et al.* (1999, 2002, and 2003) applied NN to predict wind pressure coefficients and speed-up ratios, which is also the subject of the present paper. More recently, Chen, *et al.* (2003) applied NN to predict pressure coefficients on roofs of low buildings.

In the present study, a CFD-NN approach has been used to predict a design wind load parameter: Fractional Speed-Up Ratio (FSUR) defined in terms of  $U(z)/U_o(z)$ , for different types of hill geometries where  $U(z)$  is the velocity at height  $z$  above the local hill surface,  $U_o(z)$  is the upstream reference velocity at the same height  $z$ . The emphasis is placed on the evaluation of velocity ratios since wind-induced pressures are proportional to the square of the wind speeds. Therefore, a small variation of wind speed due to the upstream topography may have a large influence on the loading of the structures. For instance, the approach used in wind loading standards, e.g., National Building Code of Canada - NBCC (1995), is to calculate the wind loading as

$$p = qC_eC_pC_g \quad (1)$$

where  $p$ : wind-induced pressure  
 $q$ : velocity pressure at a certain height  
 $C_e$ : exposure factor defining the variation of velocity pressure with height  
 $C_p$ : pressure coefficient  
 $C_g$ : gust response factor

Over flat ground the exposure factor depends only on the roughness of the terrain. To account for the influence of a hill or hills, a modified exposure factor given by

$$C'_e = C_e(z)(FSUR)^2 \tag{2}$$

where  $FSUR = U(z)/U_o(z)$  (3)

The NBCC (1995) recommends the following FSUR expression:

$$FSUR = \Delta S_{max} \left( 1 - \frac{|x|}{\kappa_1 L} \right) e^{(-\beta z/L)} + 1 \tag{4}$$

where  $\Delta S_{max}$  represents the relative speed-up ratio at the crest near the surface,  $\beta$  represents a decay coefficient for the decrease in the speed-up with height,  $\kappa_1$  represents a constant given in Table 1 and  $x$  represents the horizontal location of a position under consideration with respect to the crest of the hill. Values of  $\beta$  and  $\Delta S_{max}$  are given in Table 1.

The purpose of this study is therefore to enable the end-user to generate these FSUR values for a wide spectrum of terrain geometries easily and efficiently. Using the proposed system, FSUR values for cases such as multiple hills not covered by the NBCC (1995)-see Table 1-have been generated. Unlike previous studies, CFD results in lieu of BLWT data are used to train the NN. Ultimately, the current CFD-NN combination is shown to be less expensive (for the end-user) than BLWT studies, BLWT-NN combination or CFD simulations alone while producing results with comparable accuracy.

## 2. CFD modelling

### 2.1. Governing equations

The numerical evaluation of wind flow over topography uses CFD technique. The governing equations employed are the Reynolds Averaged Navier-Stokes (RANS) equations together with the standard  $k-\epsilon$  turbulence model (Launder and Spalding 1974) representing the turbulent wind flow over different cases of isolated and multiple hills. The vectorized form of the governing equations in a Cartesian coordinate system is as follows:

Table 1 Parameters for maximum speed-up over low hills (NBCC 1995)

Hill Shape	$\Delta S_{max}^{(1)}$	$\beta$	$\kappa_1$	
			$x < 0$	$x > 0$
2-dimensional ridges (or valleys with $H$ negative)	2.2 $H/L$	3	1.5	1.5
2-dimensional escarpments	1.3 $H/L$	2.5	1.5	4
3-dimensional axisymmetrical hills	1.6 $H/L$	4	1.5	1.5

<sup>(1)</sup>For  $H/L > 0.5$ , assume in the formula that  $H/L = 0.5$  and substitute  $2H$  for  $L$  in Eq. (4)

$$\frac{\partial E}{\partial x} + \frac{\partial F}{\partial z} = S \quad (5)$$

where

$$\begin{bmatrix} \text{continuity} \\ x\text{-momentum} \\ z\text{-momentum} \\ k\text{-equation} \\ \varepsilon\text{-equation} \end{bmatrix} E = \begin{bmatrix} \rho U \\ \rho U U - \Gamma U_x \\ \rho U W - \Gamma W_x \\ \rho U k - \Gamma k_x / \sigma_k \\ \rho U \varepsilon - \Gamma \varepsilon_x / \sigma_\varepsilon \end{bmatrix} F = \begin{bmatrix} \rho W \\ \rho U W - \Gamma U_z \\ \rho W W - \Gamma W_z \\ \rho W k - \Gamma k_z / \sigma_k \\ \rho W \varepsilon - \Gamma \varepsilon_z / \sigma_\varepsilon \end{bmatrix} S = \begin{bmatrix} 0 \\ (\mu_t U_x)_x + (\mu_t W_x)_z - P_x \\ (\mu_t U_z)_x + (\mu_t W_z)_z - P_z \\ G - \rho \varepsilon \\ (C_1 G - C_2 \rho \varepsilon) \varepsilon / k \end{bmatrix} \quad (6)$$

The subscripts  $x$  and  $z$  denote the partial derivative in the respective coordinate directions, dependent variables  $U$ ,  $W$ ,  $P$ ,  $k$  and  $\varepsilon$  represent mean velocity in  $x$ - and  $z$ -directions, pressure, kinetic energy and kinetic energy dissipation respectively. The physical quantities  $\rho$ ,  $\mu$  and  $\mu_t$  represent density, dynamic viscosity of air, and turbulent viscosity respectively.  $\Gamma$  is the sum of  $\mu$  and  $\mu_t$ . The turbulent viscosity  $\mu_t$  is given by

$$\mu_t = \rho C_\mu \frac{k^2}{\varepsilon} \quad (7)$$

The turbulent kinetic energy production rate  $G$  is expressed as

$$G = \Gamma \{ 2(U_z^2 + W_x^2) + (U_z + W_x)^2 \} \quad (8)$$

Model constants  $C_1$ ,  $C_2$ ,  $C_\mu$ ,  $\sigma_k$ ,  $\sigma_\varepsilon$  are equal to 1.44, 1.92, 0.09, 1.0 and 1.3 respectively (Launder and Spalding 1974). Eqs. (5-8) have been transformed into the general coordinate system and discretized into a system of algebraic equations. For pressure correction, Rhie and Chow's (1983) interpolation technique is adopted. Further, hybrid scheme (Spalding 1972) for convection terms and SIMPLEC iterative solution procedure of Van Doormal and Raithby (1984) for solving the dependent variables sequentially are used. For this purpose, a CFD tool has been developed on the basis of finite-volume formulation, using object-oriented approach and C++ programming language due to its better management in terms of providing, for example, clear modular structure and good frame work for source codes, and ease of reusability.

## 2.2. Boundary conditions

Log-law velocity distribution is applied along the upstream boundary. Upstream boundary values of  $k$  and  $\varepsilon$  are obtained by solving the  $k$ - $\varepsilon$  equations using inlet  $U$  and  $W$  values. In the present study, the effect of roughness has been considered throughout the ground surface of the Computational Domain (CD) in addition to incorporating its effect at the upstream boundary velocity profile. This is achieved through the computation of the shear stress, Eq. (9), throughout the ground surface and then incorporating it in the momentum equations for the ground control volumes.

$$\tau_w = \frac{U_p \mu z_p^+}{z_p \kappa \ln(z_p / z_o)} \quad (9)$$

where  $U_p = \frac{U^*}{\kappa} \ln(z_p/z_o)$  (10)

- $U^*$  : friction velocity
- $z_p$  : distance of the first grid from the ground,  $z_p^+ = \rho z_p U^* / \mu$
- $z_o$  : roughness of the ground
- $\kappa$  : Von Karman constant (= 0.4).

By taking the downstream boundary far enough from the terrain feature to be simulated, Downstream boundary  $\partial/\partial x = 0$  is assumed for all the dependent variables. Fig. 1 shows the CD and summarizes the boundary conditions. Note that  $H$  represents the height of the hill under consideration and  $L$  represents the horizontal distance from the crest to where the ground elevation is half the height of the hill.

### 2.3. Grid generation

Body-fitted and nearly orthogonal grids are used in the present study. Body-fitted grids have advantages in representing the shape of the terrain accurately. As a result the ground boundary conditions can be applied accurately. Also, the orthogonality of the grid allows nonlinear terms in the sources (S-term in Eq. 6) to be small thus stabilizing the iterative procedure. The physical location of each grid point is obtained as a solution of the partial differential equations:

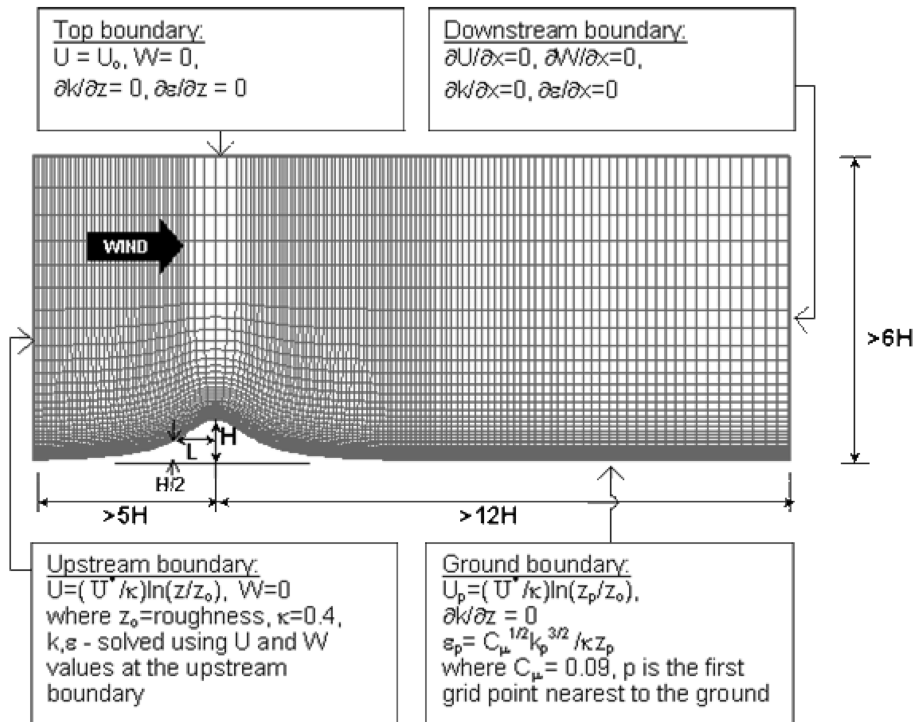


Fig. 1 Computational domain dimensions and its boundary conditions

$$(fx_\xi)_\xi + \left(\frac{1}{f}x_\eta\right)_\eta + Q(h(\xi)) + R(h(\eta)) = 0 \quad (11)$$

$$(fz_\xi)_\xi + \left(\frac{1}{f}z_\eta\right)_\eta + Q(h(\xi)) + R(h(\eta)) = 0 \quad (12)$$

where

$$h(\eta) = \sqrt{(x_\eta)^2 + (z_\eta)^2}, \quad h(\xi) = \sqrt{(x_\xi)^2 + (z_\xi)^2}, \quad (13)$$

$$f = h(\eta) / h(\xi) \quad (14)$$

$$Q(h(\xi)) = c(h(\xi) - \overline{h(\xi)})^2 / h(\xi) \quad \text{and} \quad R(h(\eta)) = c(h(\eta) - \overline{h(\eta)})^2 / h(\eta) \quad (15)$$

$$\overline{h(\xi)} = \left. \frac{\int h(\xi) d\xi}{\int d\xi} \right|_{\eta = \text{const.}} \quad \text{and} \quad \overline{h(\eta)} = \left. \frac{\int h(\eta) d\eta}{\int d\eta} \right|_{\xi = \text{const.}} \quad (16)$$

The subscripts  $\xi$  and  $\eta$  denote partial derivatives in the  $\xi$ -direction and  $\eta$ -direction respectively,  $f$  is the distortion function,  $h(\xi)$  and  $h(\eta)$  are scale factors in the  $\xi$ -direction and  $\eta$ -direction respectively, and  $c$  is a so-called force constant adjusting the magnitudes of  $Q$  and  $R$ . The distortion function has been computed numerically directly from its definition during nonlinear iterations throughout the CD, as suggested by Eca (1996). Further additional source terms  $Q$  and  $R$  suggested by Akcelic, *et al.* (2001) have also been implemented to control the scale factors favorably so that the grid points will not collapse on one another. Subsequently, the grid points have been clustered along lines connecting them in the  $\eta$ -direction as required, providing dense grid points suitable for capturing the steep gradients of the dependent variables closer to the ground. Sparse grid points have been used as well on regions of the CD away from the hill.

A collocated grid arrangement has been used in which all dependent variables  $U$ ,  $W$ ,  $P$ ,  $k$  and  $\varepsilon$  are solved at the same grid points as opposed to staggered grid; the latter is inconvenient while using body-fitted coordinates since the velocity components  $U$  and  $W$  are no longer related to the direction of grid lines. Moreover, collocated grids also ease book-keeping tasks during the computer program writing since all variables are solved at the same grid points.

The grid points are clustered densely closer to the ground boundary in order to capture the varying gradients of the dependent variables in the region. It is well documented that for near wall flow the log-law profile holds true for  $z^+ > 11$  (Bradshaw 1976), whereas for lower values it takes a linear form. The first grid point close to the ground is located so that it satisfies the log-law requirement  $z^+ > 11$ , which has been imposed for consistency with the ground boundary condition applied to the present study.

### 3. CFD results and discussion

#### 3.1. General

Wind flow over different types of topography has been simulated using the developed CFD tool over representative geometries selected to cover a wide spectrum of terrain conditions. These include

shallow and steep isolated and multiple hills. To validate or highlight the advantages or disadvantages of the currently developed numerical method, detailed comparisons are made with results obtained from five other methods: field measurements, BLWT experiments, analytical methods, NBCC provisions (1995), and existing CFD simulations, depending on availability. For the purpose of validating the developed CFD tool, the specific dimensions of the terrain geometries used are chosen in most cases to be similar to those used in the BLWT experiments reported in literature. In BLWT experiments, boundary conditions are generally better controlled, thus producing reliable and widely acceptable results by the engineering community at large.

Preliminary numerical experimentation has been conducted to select the size of the CD so that the locations of the boundaries have minimum influence on the numerical results. To study the effect of the CD height on the flow field for instance, simulations are carried out for low and high CD with height equal to  $6H$  and  $12H$  respectively, where  $H$  represents the height of the hill. The numerical results show no significant difference either in terms of mean wind velocity field throughout the CD or FSUR values above the crest of hill as shown in Fig. 2. To reduce computational time, the smaller CD height (i.e.,  $6H$ ) is used in the present study. The upstream and downstream lengths of the CD are also chosen in a similar manner as  $5H$  and  $12H$  respectively. In the case of multiple hills, the upstream length ( $5H$ ) is measured from the crest of the first upstream hill and the downstream length ( $12H$ ) is measured from the crest of the last downstream stream hill. It may be noted that for high wind speed flows, larger CD size could be necessary.

### 3.2. Isolated Hill

Under this category, wind flow over shallow and steep single cosine hills is presented. The

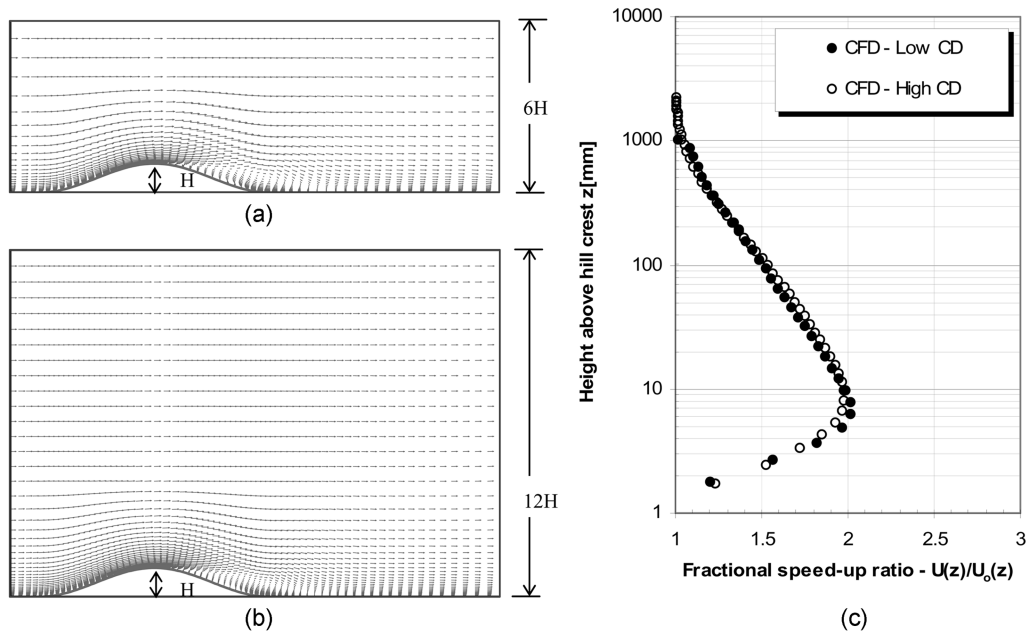


Fig. 2 Wind velocity vector field obtained by using (a) low and (b) high CD, and (c) comparison between FSUR values obtained using low and high CD ( $H = 200$  mm).

geometries and roughness parameter used are similar to those used in Carpenter and Locke's (1999) and Chung and Bienkiewicz' (2004) BLWT experiments. Thus similar to Carpenter and Locke's hills, a shallow hill with  $H = 200$  mm and  $L = 400$  mm, and a steep hill with  $H = 200$  mm and  $L = 200$  mm are used. Scaling up these dimensions by 1000 gives the actual hill dimensions. A roughness length of 0.02 m (at full scale) equivalent to open terrain category is used. A  $115 \times 36$  mesh is used both for the shallow and the steep hills. In both cases the grid extends over a CD of  $3.4 \text{ m} \times 1.2 \text{ m}$ . Numerical results are shown and compared in Figs. 3(a) and (b). In both cases, the gradual increases in velocity as the wind approaches the hills and the recirculation region behind the hills are clearly predicted. The recirculation region behind the steep hill is much larger compared to the shallow hill. For reasons of clarity, in all velocity field vector figures, the velocity vectors are plotted skipping every other grid point in the  $x$ -direction.

For validation purposes, FSUR values are compared above the crest of the hills where they are critical. The agreement between the present CFD and BLWT results is excellent for both cases of

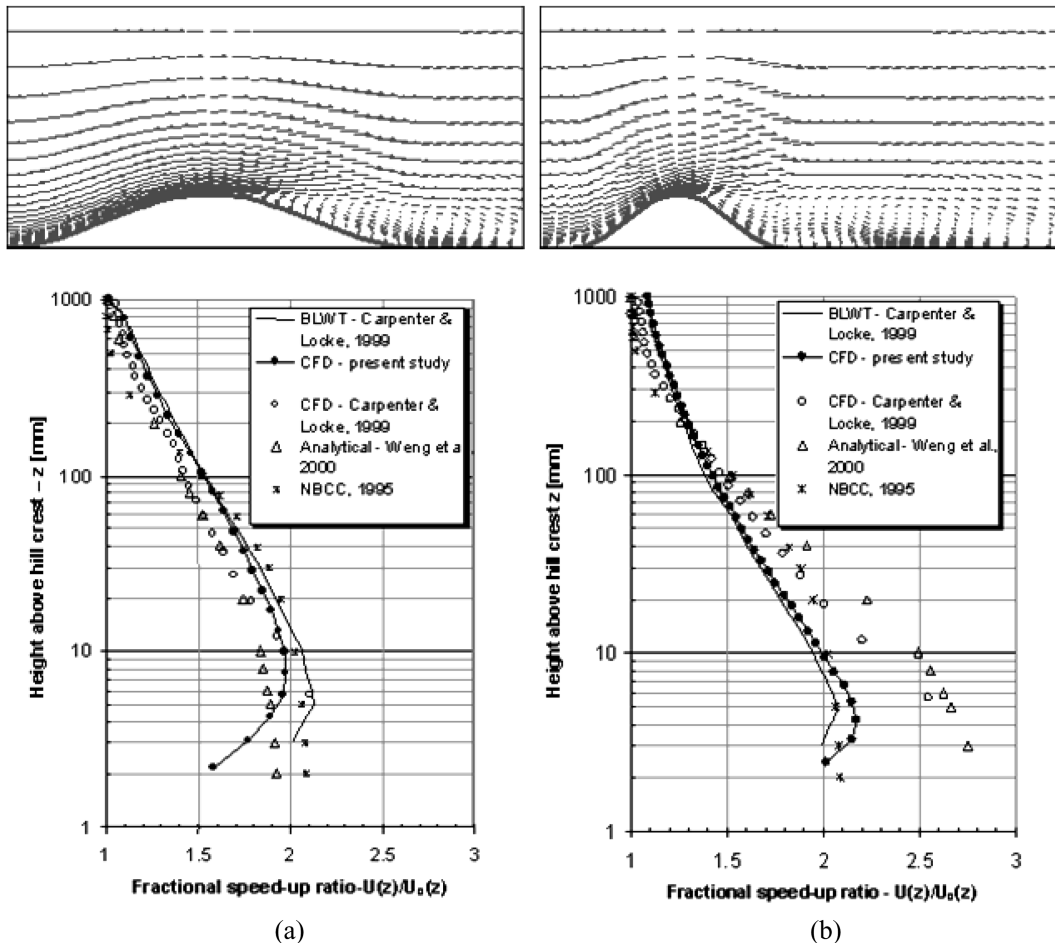


Fig. 3 Numerically obtained velocity fields (top) and comparisons (bottom) between BLWT, CFD, NBCC and analytical FSUR values above the crest of single (a) shallow, (b) steep hill ( $H = 200$  mm). All results are for two-dimensional cases.

shallow and steep hills, as shown in Figs. 3(a) and (b), respectively. In fact the present CFD simulation results agree better with the BLWT data than Carpenter and Locke's (1999) CFD data with the exception of very low heights. Amongst other factors, this close agreement is believed to be primarily due to the incorporation of roughness in the present study through the application of log law throughout the ground boundary that depicts closely the roughness conditions used by Carpenter and Locke (1999) BLWT experiments. Moreover, the body-fitted grid used in the present study allows representation of the true geometry of the BLWT model together with effective spatial distribution control of the grid points over the CD that allows a dense distribution of grid points where they are most needed. FSUR values at the crest of the hill are also generated using NBCC provisions and Weng, *et al.* (2000) guidelines, which were derived from the Multi Spectral Finite Difference (MSFD) model of Beljaars, *et al.* (1987) and its nonlinear extension (NLMSFD) by Xu, *et al.* (1994). A typical FSUR comparison between CFD, BLWT, calculated values using Weng, *et al.* (2000) guidelines and NBCC provisions (1995), is also shown in Figs. 3(a) and (b) for shallow and steep hill respectively. The agreement between CFD, BLWT, NBCC (1995) and Weng, *et al.* (2000) is good for the shallow hill. However there is sizable discrepancy among Weng, *et al.* (2000) guidelines and the BLWT data near the steep hilltop as shown in Fig. 3(b), in which the former overpredict the FSUR values. This is attributed to the inadequacy of the underlying linear theory used by the guidelines especially for wind flow over steep hills that are characterized by the presence of flow separation and large recirculation regions.

To examine the improvement in the accuracy of the present computational results due to the newly incorporated ground surface roughness, wind flow over shallow and steep single hills is also simulated with and without roughness (i.e. no slip condition on velocity) incorporation at the ground surface. For both cases, the FSUR values produced are plotted and compared with BLWT and Carpenter and Locke (1999) CFD data as shown in Fig. 4. The CFD-without-roughness shows some deviation from BLWT experiments while the CFD-with-roughness produces results closer to the BLWT data. This clearly shows that CFD result accuracy is enhanced by incorporating roughness both at the upstream velocity profile by using log law and throughout the ground boundary by enforcing roughness while calculating the shear stress for the control volumes close to the ground. It is also noteworthy to indicate that FSUR values obtained by using the present CFD-without-roughness simulations are similar to those of Carpenter and Locke (1999) CFD simulations who used similar boundary conditions, for shallow and steep cases, as can be seen on Figs. 4(a) and (b). Although both computational results deviate from BLWT values, the similarity observed among each other illustrates the repeatability of the CFD results irrespective of the formulation. It should be noted that Carpenter and Locke (1999) CFD results were obtained by using a finite element formulation.

More recently, Chung and Bienkiewicz (2004) have simulated wind flow over the steep hill shown in Fig. 5 numerically and experimentally by using BLWT tests. Comparison of FSUR values at three different longitudinal locations is shown in Figs. 6(a)-(c). The present CFD results compared very well with the experimental data both at the upstream location (i.e. at  $x = -H$ ) and at the crest (i.e. at  $x = 0$ ) of the hill. However, comparison between the two CFD studies for the downstream location (i.e. at  $x = 10H$ ) is not so good. In the present study, a large recirculation zone has been observed behind the hill when compared to the Chung and Bienkiewicz (2004) CFD simulation resulting in a rather weak agreement between the two numerical evaluations.

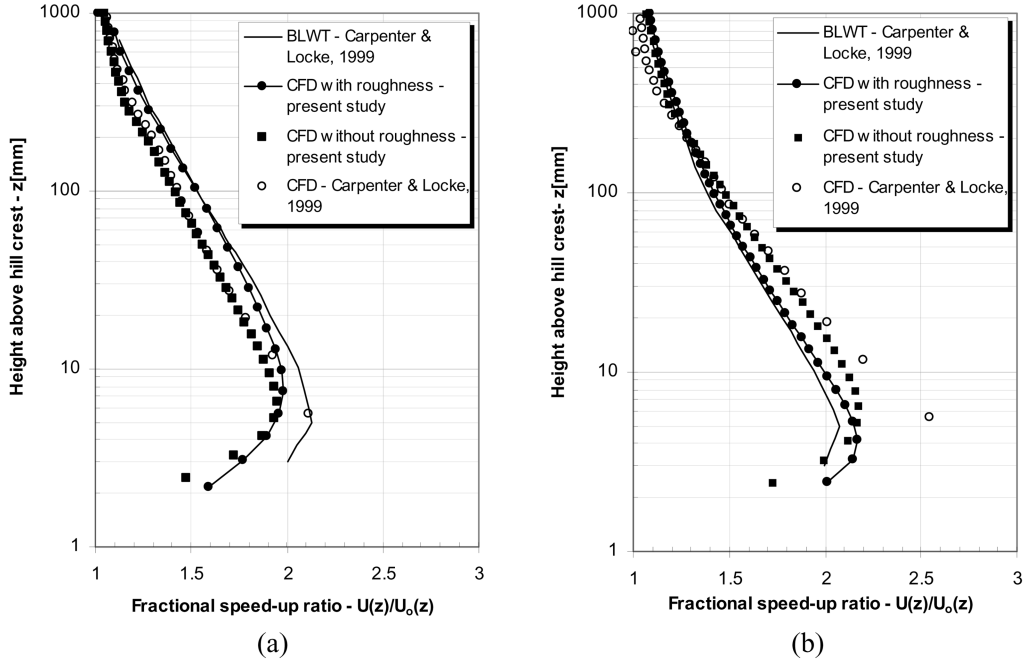


Fig. 4 Comparison between BLWT and CFD with and without roughness consideration-FSUR values above the crest of single (a) shallow and (b) steep hill

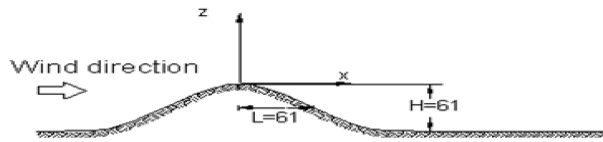


Fig. 5 Geometry used by the present as well as Chung and Bienkiewicz (2004) studies. All dimensions are in [mm]

### 3.3. 2D double hills

The geometry and roughness parameters used under this category are similar to those used in Carpenter and Locke's (1999) BLWT experiments. Thus a roughness length of 0.02 m (at full scale) is used. The shallow hills have  $H = 200$  mm and  $L = 400$  mm and the steep hills have  $H = 200$  mm and  $L = 200$  mm. Distance between the crests of the hills is  $8H$  as shown in Figs. 7(a) and 8(a). A  $179 \times 36$  mesh covering a CD of  $5.2 \text{ m} \times 1.2 \text{ m}$  is used for both the shallow and steep double hills. Figs. 7(b) and 8(b) show the mean wind velocity vectors, for the shallow and steep cases, respectively. As in the isolated hill case, the recirculation region behind the steep hills is much larger compared to the shallow case. The mean flow characteristics for double hill case however fundamentally differ from that of an isolated hill case especially for the downstream hill. This is because the wind flow separation from the upstream hill (Hill-1) results in increased turbulence on the downstream hill. This in turn causes the flow to attain more uniformity resulting in a reduction of the peak FSUR values just above the crest of the

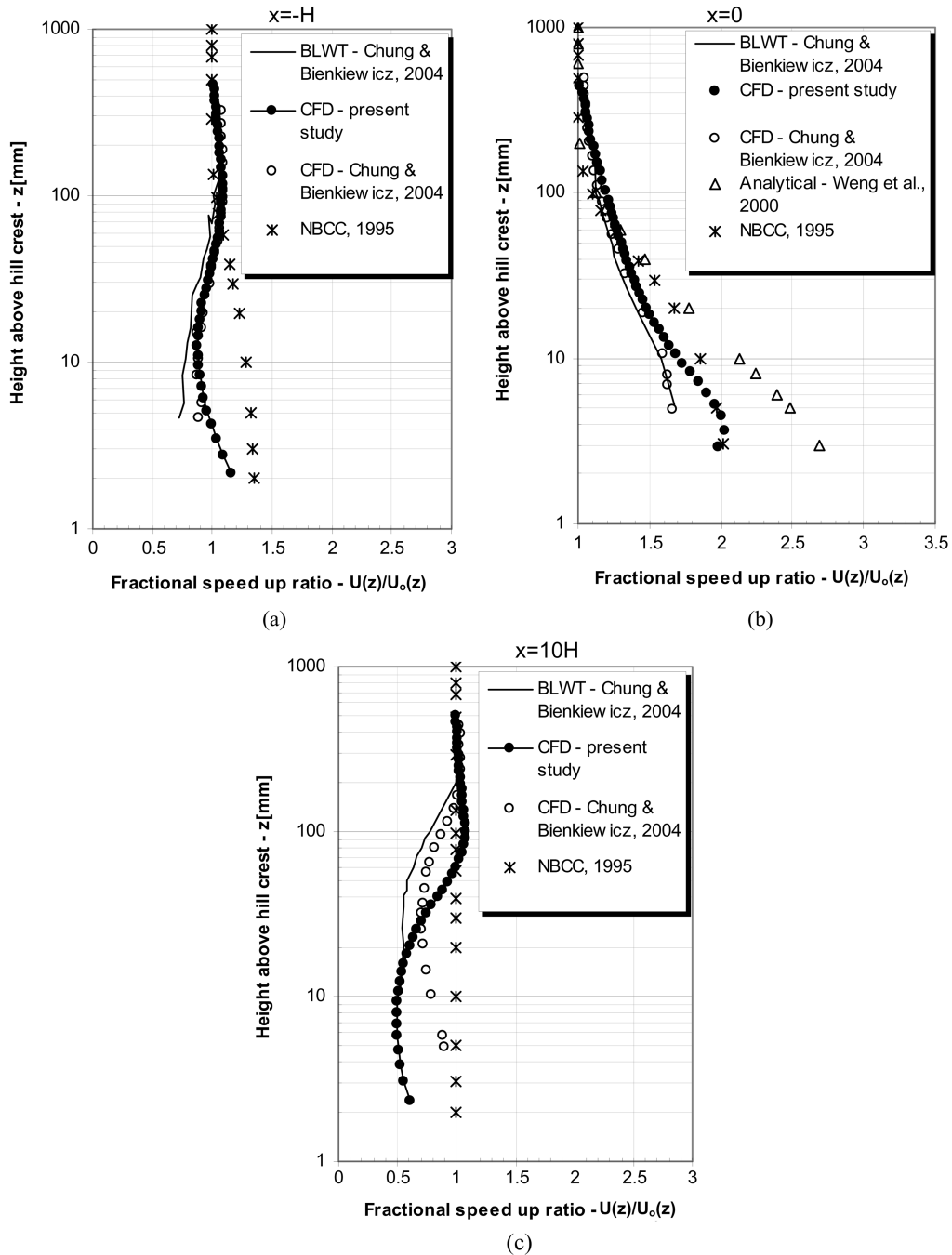


Fig. 6 Comparison between BLWT and CFD FSUR values at (a) upstream ( $x = -H$ ), (b) crest of the hill ( $x = 0$ ), and (c) downstream ( $x = 10H$ ) longitudinal locations.

downstream hill (Hill-2). Hence the FSUR values for the downstream hill (Hill-2) are smaller than the values for the upstream hill (Hill-1), as shown in Figs. 7(c) and 8(c) for shallow and

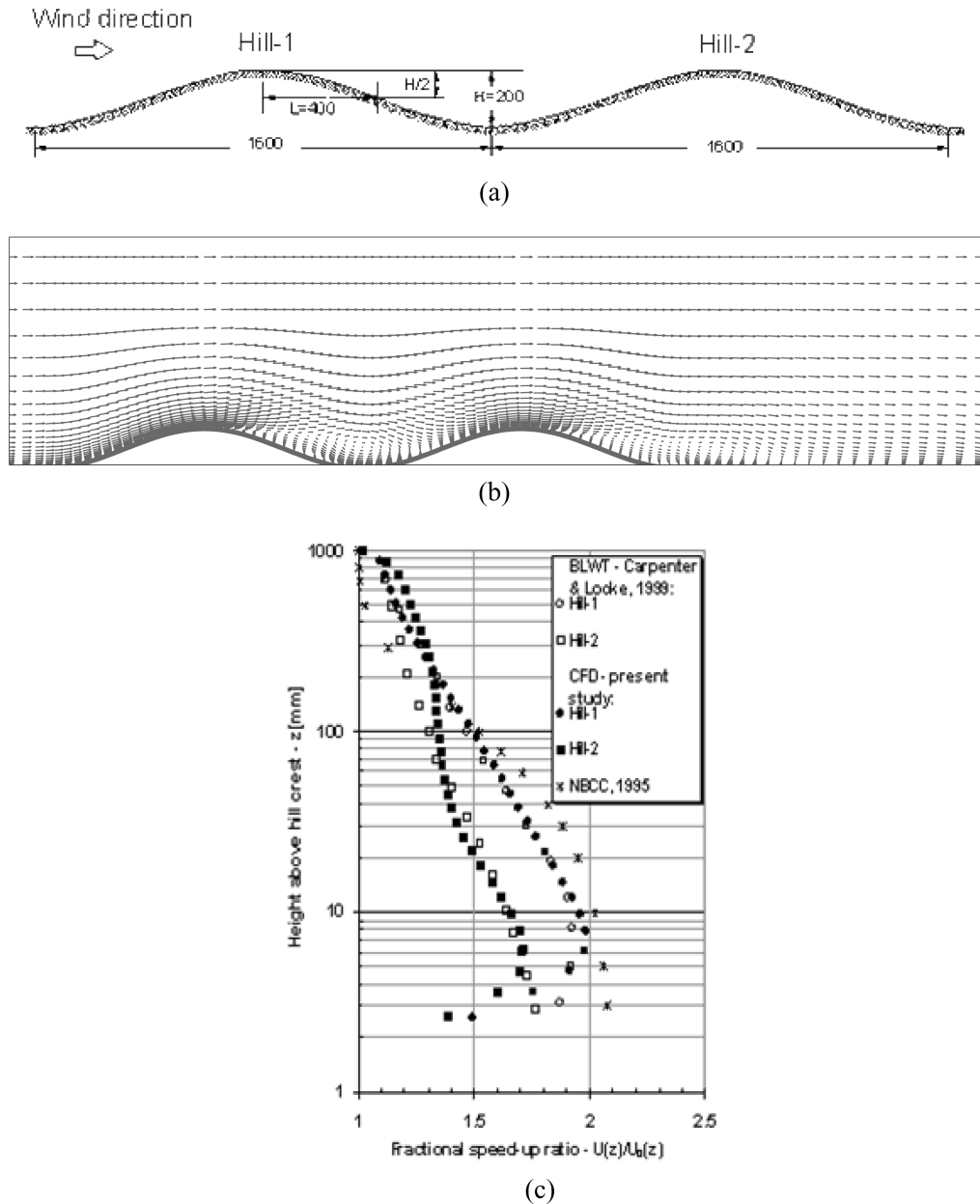


Fig. 7 Numerical simulation of wind flow over double shallow hills: (a) geometry used by the present as well as Carpenter and Locke's (1999) studies, (b) velocity field and (c) comparison between BLWT, CFD, and NBCC FSUR values above the crests. All dimensions are in [mm]

steep double hills, respectively. At the crest of the respective hills and for the height range of most engineering interest (5 – 100 m), upstream hill FSUR values are 20 to 30% larger than the downstream FSUR values for the shallow and steep double hills, respectively (Figs. 7 and 8). This percentage in terms of FSUR values can translate to approximately 45 to 70% increase in

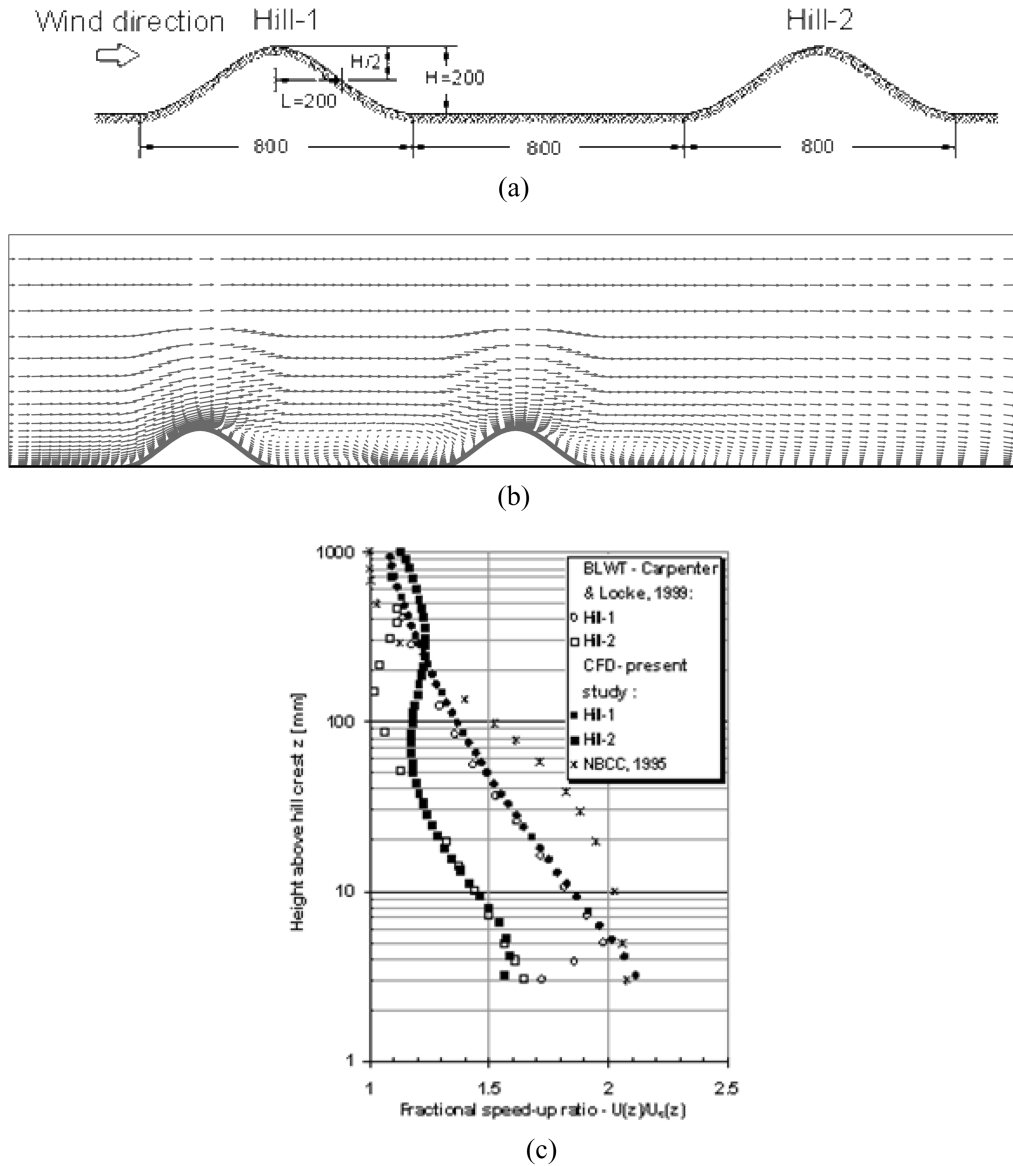


Fig. 8 Numerical simulation of wind flow over double steep hills: (a) geometry used by the present as well as Carpenter and Locke's (1999) studies, (b) velocity field and (c) comparison between BLWT, CFD, and NBCC FSUR values above the crests. All dimensions are in [mm]

wind load for the shallow and steep cases, respectively.

To date no NBCC provision (1995) exists for the case of double hills. In practice NBCC provisions for single hills apply to the double hill case. However, when NBCC provisions are used for the downstream hill case, FSUR values are overpredicted approximately by 25% and 44% for the shallow and steep hill cases respectively for the height range of 5 – 100 m. The wind load is therefore over predicted by 55% and 100% respectively. The economical impact of accurate wind load predictions has been studied by Horesfield, *et al.* (2002). It was shown that with the use of

more accurate wind loads, 19% of the concrete lateral load-resisting system (around 6500 m<sup>3</sup>) and 2.1% of usable floor area had been saved for a particular case of interest.

The practice of using identical FSUR values for both the upstream and downstream hills on the basis of the single hill investigations is indeed a conservative approach. Hence, in areas characterized by chains of mountains, the wind load has to be evaluated based on studies of multiple hills rather than single hills. In addition, the detailed wind field evaluations carried out in the present study can be of great importance in environmental planning. In an industrialized area for example, it is apparent from Figs. 7(b) and 8(b) that the recirculation zone between the hills can entrap pollutants. Furthermore considering the increasing trend of using wind energy alternatives in Canada and around the world, the present numerical simulation tool can also be useful in wind farm planning.

### 3.4. 2D triple hills

The geometry and roughness parameters used under this category are also similar to those used in Carpenter and Locke's (1999) BLWT experiments. Thus a roughness length of 0.02 m (full scale) corresponding to open terrain category has been simulated. The shallow hills have  $H = 200$  mm and  $L = 400$  mm and the steep hills have  $H = 200$  mm and  $L = 200$  mm. Distance between the crests of the hills is  $8H$ . A  $243 \times 36$  mesh covering a CD of  $6.5 \text{ m} \times 1.2 \text{ m}$  is used for both the shallow and steep triple hills.

In Carpenter and Locke (1999), BLWT experiments show the highest crest FSUR values were observed at the crest of upstream hill (Hill-1), and the second largest at the crest of downstream hill (Hill-3) while the smallest FSUR values occurred at the crest of the middle hill (Hill-2), for both shallow and steep triple hill cases. It is interesting to see the same patterns of FSUR values as observed in the BLWT experiments being captured by the CFD simulations, as shown in Figs. 9(a) and (b) for shallow and steep triple hills, respectively. This is with the exception of FSUR values for Hill-2 and Hill-3 of the shallow hills which are identical as shown in Fig. 9(a). This type of variation of FSUR values over the three hills is due to the flow separation from the first hill, resulting in low wind speeds and increased turbulence at the second hillcrest. This increased turbulence at the second hillcrest helps to reduce the flow separation from the second hill and so the mean speed at the third hillcrest increases relative to that at the second hillcrest.

Overall there is good agreement between CFD and BLWT experimental data for triple shallow hills as shown in Fig. 9(a). Comparison of FSUR values for steep triple hill case with BLWT data at the hillcrests shown in Fig. 9(b) indicates that CFD predicted FSUR values are in good agreement for the upstream hill (Hill-1) and middle hill (Hill-2), whereas for the last downstream hill (Hill-3), ratios are relatively smaller than BLWT values but still in better agreement than NBCC provisions (1995). Note that the maximum of the FSUR values at Hill-1 for steep hill case did not occur exactly at the hillcrest but one grid point upwind (15 mm) of the crest due to the effect of flow separation closer to the hillcrest. In similar situations in the present study, these FSUR values have been used.

Generally, NBCC values for the isolated hill cases agree with both BLWT and CFD predictions as discussed in the previous sections; however no provisions are given for the cases of multiple hills. The application of NBCC FSUR values specified for single hills directly to the case of multiple hills is a conservative approach. For example, NBCC (1995) would have over-predicted the fractional speed-up ratios by 47% and 43% for shallow Hill-2 and shallow Hill-3 respectively at 40

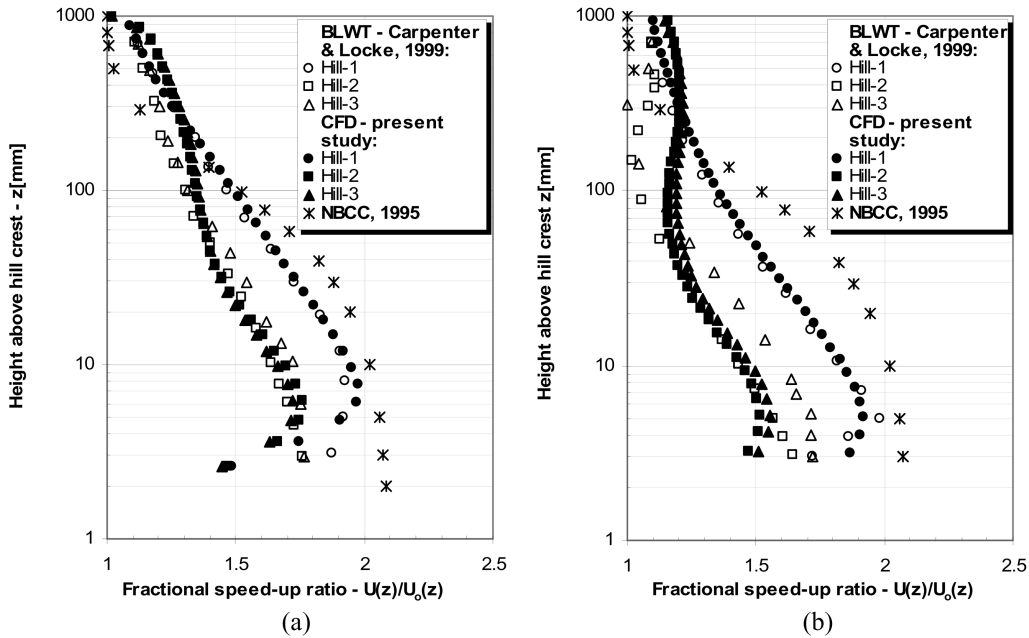


Fig. 9 Comparison between FSUR values obtained from BLWT, CFD and NBCC above the crest of (a) shallow and (b) steep triple hills.

m above the hillcrest. This can be translated to an increase of wind load in the order of approximately 100%. As pointed out previously, the economical impact of wind load prediction accuracy is very significant for such cases.

#### 4. CFD-NN approach

Neural Networks are data driven models useful for mapping non-linear relationships that exist in wind flow data. In NN modeling two processes, i.e., learning and prediction/testing, are performed. During the learning process, the NN basically learns from a representative training data set containing both input parameters (identified to be influential) and output parameters. In the present case, the input includes geometrical and roughness parameters of the terrain. The output consists of the FSUR value. The NN “learns” how to map input parameters into an output parameter through an iterative process that involves optimization and other simple mathematical operations (Khanduri, *et al.* 1995). Once the learning process is completed, the trained NN can be used to generate FSUR values for new cases either through interpolation or extrapolation. For the NN modeling to be successful, representative training data is required. Training data can be obtained by running BLWT tests. In the present study a computational approach has been adopted instead, mainly for economical reasons. This proposition is particularly attractive when current trends in the improvement of hardware/software technology together with lower costs are taken into perspective. The computational approach used to generate the training data is based on numerical solutions by using CFD techniques. Thus CFD replaces the traditional role of BLWT experimental studies.

One may ask the questions “why use NN, why not CFD only?” The answer is straightforward: although CFD-based numerical solutions may require less resources compared to BLWT

experiments, they are rarely simple and require considerable computational time, background knowledge and experience. CFD simulations require a number of tasks: solving for each dependent variable iteratively, which typically involves solving tens of thousands equations (for two dimensional cases) iteratively, using appropriate flow governing equations and the selection of a turbulence model, dealing realistically with boundary conditions for each dependent variable, finding an accurate geometrical representation of the terrain by means of good quality grid generation as well as optimal relaxation parameters for each dependent variable. In contrast, with the proposed CFD-NN approach, only the final trained NN is presented to the end-user. With simple geometry parameters and hill roughness, this model can generate the design parameter of interest using fast and simple mathematical calculations with no iterations on a personal computer. Thus the proposed CFD-NN approach is less expensive for the end-user than CFD simulations alone. It is also less expensive than the BLWT-NN combination while producing results of comparable quality.

Along this line it is worth mentioning the work of Lemelin, *et al.* (1988) and Weng, *et al.* (2000), who provided useful simple approximations for wind speed-up based on data obtained from computational and a combination of computational and BLWT tests respectively. However, such approaches have limitations. For instance, Lemelin, *et al.* (1988) did not consider the effect of roughness on speed-up and the computational data used to derive the model assumed only linear effects (Taylor, *et al.* 1983). As a result, the model works only for gentle slope isolated hill cases and deviates considerably from BLWT results when used for steep and multiple hill cases (Bitsuamlak, *et al.* 2004, Bitsuamlak 2004). Weng, *et al.* (2000) on the other hand, regressed their model based on data obtained from the non-linear extension of the theoretical model (Taylor, *et al.* 1983, Xu, *et al.* 1994). Their model includes the effect of roughness as well, but limited only for applications at the crest of single hills. In the present approach, a CFD-neural network model, incorporates roughness and can be used both for steep single and multiple hills. In addition, it is very flexible to incorporate new influential parameters into the model when available. One such case is future incorporation of the fluctuation part of the wind flows to estimate the gust components of wind loads. In this regard the authors are working on generating fluctuating components of wind flow using a more complex turbulence model such as Large Eddy Simulation (LES).

The proposed CFD-NN approach uses the following steps in order to produce the trained NN:

1. Training data is generated using the proposed CFD tool. Hill geometries similar to those used in previous CFD and BLWT studies are used.
2. CFD-generated values are validated by comparison with existing BLWT and CFD data.
3. NN is trained using CFD-generated training data.
4. NN-generated data is validated by comparison with existing BLWT and CFD data.

The trained NN is used to generate new wind design load parameters. Note that finally it is this trained NN that will be provided to the end user.

The schematic shown in Fig. 10 summarizes the proposed CFD-NN system. The “CFD model” has been discussed previously in this paper. The second component, namely “NN model” is discussed in the following sub-sections.

#### 4.1. NN modelling

A NN tool has been developed using C++ programming language for prediction of FSUR values.

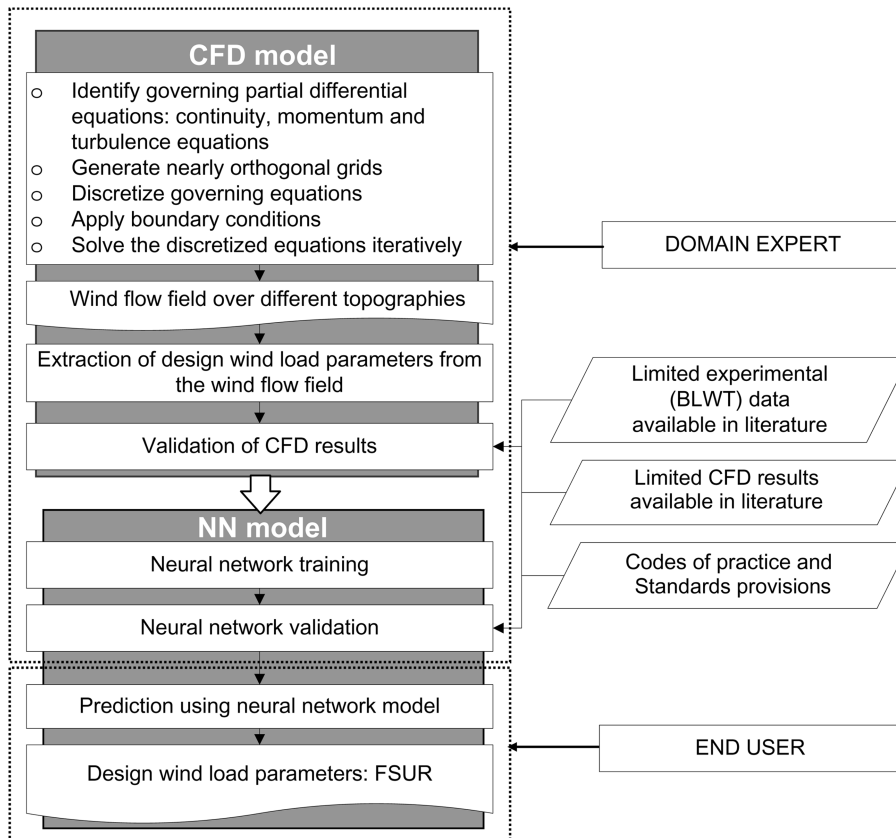


Fig. 10 Schematic development of the proposed CFD-NN system

The NN is based on the cascade-correlation-learning algorithm of Fahlman and Lebiere (1990) chosen due to its automatic determination of its topology, incremental learning and a higher level of interconnections. In addition to the regular input to hidden layer connections and hidden to output layer connections that exist in the standard back-propagation NN (Khanduri, *et al.* 1997), there are connections among hidden neurons and between input and output neurons as well. Each hidden neuron acts as a hidden layer, receiving input from input neurons and preexisting hidden neurons, facilitating more communication between hidden neurons and also leading to the creation of very powerful higher-order non-linear models. The architecture of the CCNN is shown in Fig. 11. New hidden neurons are installed during run-time in the active network as required from a pool of candidate-hidden neurons that are trained at the background to give maximum correlation with the output. This is unlike the standard back-propagation NN in which the number of hidden neurons is determined by trial and error before run-time. Khanduri, *et al.* (1995) reported that determining the NN architecture a priori by trial and error was one of the major problems faced while building a neural network advisor for interference effects on building wind loads using standard back-propagation NN. The developed NN tool “freezes” also some of the neurons during training to prevent them from behaving identically and from a moving target problem. Connections shown with solid lines in Fig. 11 are frozen once the hidden neurons are installed in the active network. The broken line connections however are trained repeatedly. This strategy allows the NN to learn faster.

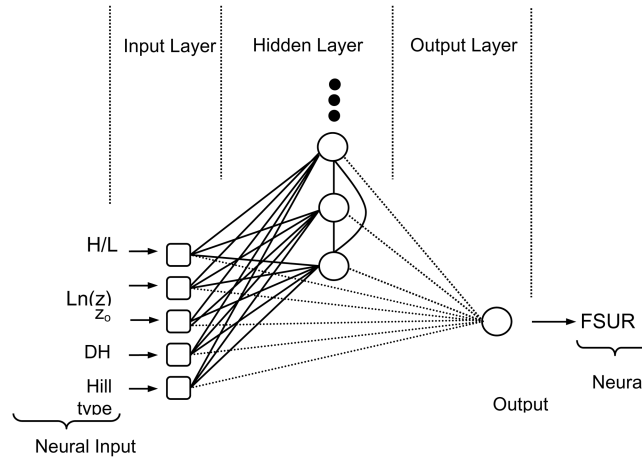


Fig. 11 A NN with cascade-correlation architecture after three hidden neurons have been added

#### 4.2. Training data description

Representative training data is crucial for successful application of NN models. Finding data that represents the different scenarios in a problem is the major challenge in NN applications for engineering purposes in general and wind engineering in particular. This requires considerable efforts as well as resources. In the present study, training data is generated by using the CFD tool described in the previous section, thus making the whole procedure a numerical process. Generally, this approach requires fewer resources as compared to generating training data using BLWT experiments. In fact, for the end user, it is also faster and cheaper than running the CFD simulation alone. With the CFD-NN approach, the end user is provided with a trained NN. Since the NN learns relationships directly from training data, one has to ensure their quality prior to their use. In the present case, CFD data generated and validated in the previous sections for shallow ( $H/L = 0.5$ ) and steep ( $H/L = 1$ ) and triple hills has been used to train the NN. For the case of multiple hills, distances between hills equal to  $8H$  and  $6H$  have been used. Both smooth ( $z_o = 0.002$  m) and rough ( $z_o = 0.016$  m) hill surfaces are considered in the training data. In the present study, each case contains approximately 40 data points.

#### 4.3. Input/Output parameter identification

Sets of input and output parameters are required to train the neural network. As much as possible the input variables should include all the parameters that are known to influence the output parameter. In the present case, the output parameter is the FSUR value. As seen previously, FSUR values depend on several parameters. In order to train and test the NN, it is therefore necessary to develop data sets consisting of FSUR values in relation to the various relevant input parameters. After thorough investigation, and with the help of the knowledge gained from CFD simulations and from experience, the following parameters are selected as input to the NN:

1. Geometrical parameters:
  - Windward slope of the hill:  $H/L$ .

- Height from the crest of the hill at which FSUR values are to be determined -  $\ln(z)$ . Since variations are significant closer to the ground, a logarithmic scale has been adopted instead of a normal scale ( $z$ ).
  - Distance between hills in case of multiple hills:  $DH$ .
2. Roughness length of the ground:  $z_o$ .
  3. Hill type: single, multiple. For the case of multiple hills a parameter that enables the NN to identify each hill is required. For this purpose an arbitrary hill count coefficient has been defined in the following manner: (1,0,0), (0,1,0) and (0,0,1) for upstream, middle and downstream hill of the triple-hill case respectively.

Input and output parameters are also shown in Fig. 11. Five input neurons have been used in the input layer. The expected output from the CCNN is only the FSUR value; hence a single output neuron has been used in the output layer. The number of hidden neurons is determined during run time automatically. In the present case 11 hidden neurons have been used.

#### 4.4. CFD-NN results and discussion

During the training phase, the CCNN learns iteratively how to map the geometric parameters and the roughness into corresponding FSUR values. The trained CCNN has 11 hidden neurons. Once the training is over, the trained CCNN is tested first for reproducing the CFD results of the same case, and then for predicting FSUR values for a new hill geometry that has not been considered during the training phase. This reproduction test is carried out for the single shallow ( $H/L = 0.5$ ) and steep ( $H/L = 1$ ) hills. As one may expect this exercise was not challenging to the CCNN, which reproduced the CFD data exactly with R-square value of 1. It has also shown good agreement with Carpenter and Locke (1999) BLWT data. However this simple exercise shows that a NN can provide the end user with CFD-like results using simple input parameters and fewer mathematical computations. The second test was carried out for a new case of intermediate triple hill ( $H/L = 0.66$ ) that was not considered during the training phase. The predicted FSUR values are consequently compared with Miller (1996) BLWT data as shown in Fig. 12. The CCNN FSUR values agree very well with the BLWT data and they capture as well the decrease in FSUR values for the downstream hills as shown in Fig. 12. R-square values between NN and BLWT FSUR values equal to 0.99, 0.99 and 0.96 have been obtained for Hill-1, Hill-2 and Hill-3 respectively. Fig. 12 also shows comparisons between NBCC and BLWT FSUR values for the same geometries. Although the NBCC FSUR values agree with the BLWT data for the upstream hill (Hill-1), their use for the downstream hills will overpredict FSUR values. The use of NBCC-1995 provisions yields R-square values equal to 0.92, 0.85 and 0.86 for Hill-1, Hill-2 and Hill-3 respectively. The NN-BLWT R-square values are better than NBCC-BLWT R-square values by 7.5%, 14% and 11% for Hill-1, Hill-2 and Hill-3 respectively. This shows that a considerable improvement in the accuracy of FSUR evaluation can be achieved by using the CFD-NN approach. It also indicates that the CCNN not only reproduces the CFD result accurately but also generates reliable FSUR values for new hill geometries. It has to be noted that, this study is only an illustration of this new CFD-NN methodology. In practical application, more training data has to be generated representing a wide spectrum of terrain types and used to train the neural network. As a rule of thumb, a 3:1 training versus application ratio is suggested to decide the training data size.

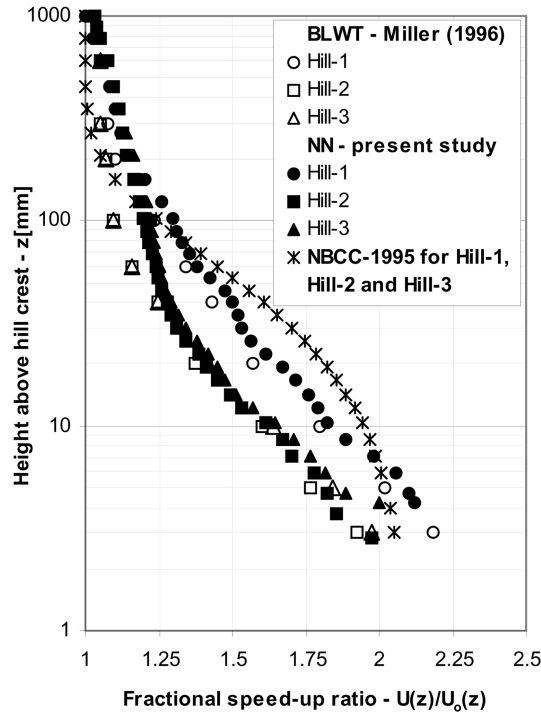


Fig. 12 Comparisons of FSUR values at the crest of triple hills ( $H/L = 0.66$ ) obtained using NN, BLWT, and NBCC

## 5. Conclusions

The paper demonstrates that CFD can be used to predict fractional speed-up ratios above different topographies, mainly simple and multiple hills with different ground roughness. A CFD-NN approach useful for estimating design wind loads on buildings in the vicinity of hills has been developed and validated. Consistent FSUR ratio values are generated using the developed CFD code, which are consequently used to train the CCNN. Their comparison with experimental values depicts a good agreement over different hill geometries of the test data range. The CCNN FSUR predictions also indicate good agreement with the experimental data both for single and multiple hills. Compared to CFD simulation, the use of NN models does not require expensive computational time or hardware. In addition, the NN approach requires only simple hill geometrical parameters and roughness of the ground to produce the corresponding FSUR values. The trained NN can be distributed among practicing engineers and can be easily used to estimate the variation in wind load due to upstream hills. The present CFD-NN approach has also been applied successfully for multiple hill geometries not currently addressed in wind codes and standards.

## References

- Akcelik, V., Jaramaz, B. and Ghattas G. (2001), "Nearly orthogonal two-dimensional grid generation with aspect ratio control", *J. Comput. Physics*, **171**, 805-821.
- Bejaars, A.C., Walmsley, J.L. and Taylor, P.A. (1987), "A mixed spectral finite-difference model for neutrally

- stratified boundary-layer flow over roughness changes and topography”, *Boundary-Layer Meteorology*, **38**, 273-303.
- Bergeles, G.C. (1985), “Numerical computation of turbulent flow around two-dimensional hills”, *J. Wind Eng. Ind. Aerodyn.*, **21**, 307-321.
- Bitsuamlak, G.T. and Godbole, P.N. (1999), “Application of cascade-correlation learning network for determination of wind pressure distribution in buildings”, *Wind Engineering into the 21st Century*, Balkema, Rotterdam, 1493-1496.
- Bitsuamlak, G.T., Stathopoulos, T. and Bédard, C. (2002), “Neural network predictions of wind flow over complex terrain”, *4<sup>th</sup> Structural Specialty Conference of the Canadian Society for Civil Engineering*, Montréal, Québec, Canada, ST-026, S-13.
- Bitsuamlak, G.T., Stathopoulos, T. and Bédard, C. (2003), “Numerical evaluation and neural net predictions of wind flow over complex terrain”, *11<sup>th</sup> International Conference on Wind Engineering*, June 2-5, Lubbock, Texas, USA, **2**, 2673-2679.
- Bitsuamlak, G.T., Stathopoulos, T. and Bedard, C. (2004), “Numerical evaluation of wind flow over complex terrain: Review”, *J. Aerospace Eng.*, **17**(4), 135-145.
- Bitsuamlak, G.T. (2004), “Evaluating the effect of topographic elements on wind flow: A combined numerical simulation-neural network approach”, Ph.D. Thesis, Concordia University, Montreal, Canada.
- Bradshaw, P. (1976), “Topics in applied physics-turbulence”, **12**, Springer-Verlag, NewYork, 2nd Ed.,
- Carpenter, P. and Locke, N. (1999), “Investigation of wind speed over multiple two-dimensional hills”, *J. Wind Eng. Ind. Aerodyn.*, **83**, 109-120.
- Chen, Y., Kopp, G.A. and Surry, D. (2003), “Prediction of pressure coefficients on roofs of low buildings using artificial neural networks”, *J. Wind Eng. Ind. Aerodyn.*, **91**, 423-441.
- Chung, J. and Bienkiewicz, B. (2004), “Numerical simulation of flow past 2D hill and valley”, *Wind and Struct., An Int. J.*, **7**(1), 1-12.
- Eca, L. (1996), “2D orthogonal grid generation with boundary point distribution control”, *J. Comput. Physics*, **125**, 440-453.
- English, E.C. and Fricke, F.R. (1999), “The interference index and its prediction using a neural network analysis of wind-tunnel data”, *J. Wind Eng. Ind. Aerodyn.*, **83**, 567-575.
- Fahlman, S.E. and Lebiere, C. (1990), “The cascade correlation learning architecture”, *D.S. Touretzky, Advances in Neural Information Processing Systems II*, Morgan Kaufmann, 524-532.
- Horsfield, J.N., Chan, C.M. and Denoon, R.O. (2002), “Towards sustainable development through innovative engineering”, *Housing Conference*, Wanchai, Hong Kong.
- Khanduri, A.C., Bedard, C. and Stathopoulos, T. (1995), “Neural network modelling of wind-induced interference effects”, *Proceedings of the Ninth International Conference on Wind Engineering*, New Delhi, India, 1341-1352.
- Khanduri, A.C., Bedard, C. and Stathopoulos, T. (1997), “Modelling wind-induced interference effects using backpropagation neural networks”, *J. Wind Eng. Ind. Aerodyn.*, **72**, 71-79.
- Launder, B.E. and Spalding, D.B. (1974), “The numerical computation of turbulent flows”, *Comput. Methods Appl. Mech. Eng.*, **3**, 269-289.
- Lun, Y.F., Mochida, A., Yoshino, H., Murakami, S. and Kimura, A. (2003), “Applicability of linear type revised  $k-\epsilon$  models to flow over topographic feature”, *11<sup>th</sup> International Conference on Wind Engineering*, June 2-5, Lubbock, Texas, USA, **2**, 1149-1156.
- Lemelin, D.R., Surry, D., and Davenport, A.G. (1988), “Simple approximations for wind speed-up over hills”, *J. Wind Eng. Ind. Aerodyn.*, **28**, 117-127.
- Maurizi, A., (2000), “Numerical simulation of turbulent flows over 2D valleys using three versions of the  $k-\epsilon$  closure model”, *J. Wind Eng. Ind. Aerodyn.*, **85**, 59-73.
- Miller, C.A. (1996), “Turbulent boundary layers above complex terrain”, Ph.D. thesis, University of Western Ontario, London, Ontario, Canada.
- NBCC, National Building Code User’s Guide-Structural Commentaries (Part 4), Canadian Commission on Building and Fire Codes, National Research Council of Canada, Ottawa (1995).
- Paterson, D.A. and Holmes, J.D. (1993), “Computation of wind flow over topography”, *J. Wind Eng. Ind. Aerodyn.*, **46&47**, 471-478.

- Rhie, C.M. and Chow, W.L. (1983), "Numerical study of the turbulent flows past an airfoil with trailing edge separation", *AIAA J.*, **21**, 1525-1532.
- Sandri, P. and Mehta, K.C. (1995), "Using backpropagation neural network for predicting wind-induced damage to building", *Proceedings of the Ninth International Conference on Wind Engineering*, New Delhi, India, 1989-1999.
- Spalding D.B. (1972), "A novel finite-difference formulation for differential expressions involving both first and second order derivatives", *Int. J. Num. Methods Eng.*, **4**, 551-559.
- Taylor, P.A., Walmesly J.L. and Salmon, J.R. (1983), "A simple model of neutrally stratified boundary-layer flow over real terrain incorporating wave number dependent scaling", *Boundary-Layer Meteorol.*, **26**, 169-189.
- Van Doormal, J.P and Raithby, G.D. (1984), "Enhancements of the SIMPLE method for predicting incompressible fluid flows", *Numer. Heat Transfer*, **7**, 147-163.
- Weng, W., Taylor, P.A. and Walmsley, J.L. (2000), "Guidelines for airflow over complex terrain: Model developments", *J. Wind Eng. Ind. Aerodyn.*, **86**, 169-186.
- Xu, D., Ayotte, A.W. and Taylor, P.A. (1994), "Development of a non-linear mixed spectral finite difference model for turbulent boundary-layer flow over topography", *Boundary-Layer Meteorol.*, **70**, 341-367.